Directional asymmetry of the nonlinear wave phenomena in a three-dimensional granular phononic crystal under gravity

A. Merkel, V. Tournat, and V. Gusev
LUNAM Université, Université du Maine, CNRS, LAUM UMR 6613, Avenue Olivier Messiaen, 72085 Le Mans, France
(Received 25 April 2014; published 25 August 2014)

We report the experimental observation of the gravity-induced asymmetry for the nonlinear transformation of acoustic waves in a noncohesive granular phononic crystal. Because of the gravity, the contact precompression increases with depth inducing space variations of not only the linear and nonlinear elastic moduli but also of the acoustic wave dissipation. We show experimentally and explain theoretically that, in contrast to symmetric propagation of linear waves, the amplitude of the nonlinearly self-demodulated wave depends on whether the propagation of the waves is in the direction of the gravity or in the opposite direction. Among the observed nonlinear processes, we report frequency mixing of the two transverse-rotational modes belonging to the optical band of vibrations and propagating with negative phase velocities, which results in the excitation of a longitudinal wave belonging to the acoustic band of vibrations and propagating with positive phase velocity. We show that the measurements of the gravity-induced asymmetry in the nonlinear acoustic phenomena can be used to compare the in-depth distributions of the contact nonlinearity and of acoustic absorption.

DOI: 10.1103/PhysRevE.90.023206 PACS number(s): 43.25.+y, 45.70.−n, 62.30.+d

I. INTRODUCTION

Asymmetric acoustic wave propagation is of major interest for wave propagation control and its ultrasonic applications. This phenomenon can lead to the design of acoustic diode or acoustic rectifier [1–6]. Asymmetric acoustic wave propagation can be obtained with a graded phononic structure [7], a combination of two nonlinear layers [8], a combination of phononic effects with nonlinearity [2–4,9], or diffraction [10]. Noncohesive granular phononic crystals offer interesting perspectives in this topic due to the combination of the periodicity of the structure leading to phononic effects [11–22] with a highly nonlinear behavior of granular materials [16,23–27]. A noncohesive granular phononic crystal is a periodic arrangement of monodisperse elastic beads. The nonlinearity comes from the microscopic level of the contacts between the beads which in some cases is well described by the Hertz-Mindlin theory of contact between two spheres [28,29]. For instance, the acoustic properties of granular crystals can be controlled by an external static loading that can change the spectrum of bulk modes propagating inside of them [15,17–19,30]. Recently, the combination of the phononic effects with a nonlinear effect around a localized breather has been used to observe an important rectification effect in a one-dimensional granular crystal with defect [4,31,32]. It has been also demonstrated that the asymmetry in the defect position in the chain can induce the asymmetry in the propagation of acoustic waves.

In three-dimensional noncohesive granular media, the translational symmetry is actually always naturally broken along the direction of the gravity field, because the static loading on the contacts between the beads and, as a consequence, their rigidities, increase along the gravity direction [33]. It has been earlier demonstrated that this gravity-induced inhomogeneity of the elastic properties in the vertical direction induces acoustic waves guided along the mechanically free surface of the granular assemblies [34–36] and in subsurface channels [37]. Here, we demonstrate how the gravity introduces asymmetry in the vertical propagation of nonlinear acoustic waves by inducing an in-depth inhomogeneity of the linear and nonlinear elastic parameters.

We experimentally reveal and theoretically interpret the asymmetry introduced by the gravity in the three-wave mixing down-conversion processes in a three-dimensional granular crystal. We excite acoustic wave packets, i.e., high frequency signals centered within a narrow frequency band, in the granular crystal from its surface. We detect low frequency waves with frequencies of the order of the width of the wave packet in frequency, which are nonlinearly generated in the bulk of the granular crystal. In others words, we are using for the diagnosis of the vertical propagation of acoustic waves in granular crystals the nonlinear parametric emitting antenna phenomenon [38]. Earlier, the demodulation, or rectification, effect of acoustic wave packets has been experimentally studied in disordered granular media [24,39,40]. The parametric emitting antenna has been theoretically studied in disordered granular media [41,42] and in a one-dimensional monoatomic granular chain [43].

In our experiment in the three-dimensional granular crystal, the amplitude of the demodulated acoustic wave is detected from two different paths of propagation. For the first path, the wave packet is emitted at the top of the crystal, the propagation is therefore along the gravity direction, i.e., "from top to bottom" (downward) ↓-propagation. For the second path, the wave packet is emitted at the bottom of the crystal, the propagation is along the direction opposite to the gravity, i.e., "from bottom to top" (upward) ↑-propagation. The detected amplitudes of the demodulated waves from the two different paths differ. The directional asymmetry is documented both in parametric emission with mode conversion from rotational-transverse wave packets into longitudinal acoustic pulses and in parametric emission without mode conversion from longitudinal wave packets into longitudinal demodulated pulses. It is worth noting that, in the first case, the frequency down-conversion process is observed for an acoustic wave with opposite directions of the phase and group velocities. We also observe that the sign of the directional asymmetry, i.e., the parameter indicating which one

of the propagation directions leads to more efficient parametric emission, depends on the central frequency of the acoustic packets. We provide qualitative physical explanations for all the observed phenomena.

From the physical point of view, the amplitude of the demodulated wave depends, for a fixed amplitude of the wave packet in excitation, on the efficiency of the interaction between the high frequency components of the acoustic spectrum and on the effective amplification length of low acoustic frequencies by high frequencies [38,40–44]. Interaction efficiency is proportional to the nonlinear acoustic parameter and can depend on frequency. Theoretically, the amplification length, i.e., the length of the parametric antenna, can be controlled by absorption, dispersion, diffraction, and nonlinearity of the acoustic propagation in the medium. We argue that, in our experiments, the directional asymmetry of the demodulation phenomenon is due to the influence of the depth-dependent static loading of the contacts between the grains either on the nonlinear acoustic parameter only or both on the nonlinear acoustic parameter and on the length of the parametric antenna.

The paper is structured as follows. In Sec. II, we present the experimental setup and remind the theoretical predictions of the dispersion curves of the different modes of linear propagation. The experimental results are presented in Sec. III. In Sec. IV, we provide qualitative explanations of the documented phenomenon of the directional asymmetry. A simplified mathematical model of the parametric emission in inhomogeneous media, which supports our qualitative interpretations of the experimental results, is described in Sec. V, followed by the discussion and conclusions.

II. EXPERIMENTAL SETUP

The experimental setup, exposed in Fig. 1, is basically the same as the one used earlier for the demonstration of the rotational elastic mode propagation in a granular phononic crystal [19]. A hexagonal closed-packed (hcp) crystal of 27 layers of noncohesive stainless steel beads is built inside a Plexiglas cell of an equilateral triangular base in which an exact number of particles fits in the first layer. The crystalline structure considered here is stable with gravity and easy to build. This structure is a vertical stacking of hexagonal layers A and B, which are in the closest position relative to each others, in a ABAB...sequence [18]. The bottom of the container is an aluminum plate with an imprint of a hexagonal lattice. The diameter a of the beads is $a = 2$ mm and the vertical distance of propagation is $H = 44$ mm. The Young's modulus of the stainless steel is 200 GPa, the mass density is 7780 kg m^{-3}, and the Poisson's ratio is 0.3. The crystal is carefully built layer by layer removing manually the geometrical defects. The acoustic waves are generated and detected by nominally shear transducers. A static loading is applied on the crystal resulting in forces from $N_0 = 2$ mN to $N_0 = 25$ mN per contact. Even in macroscopically ordered structures, disorder exists at the microscopic level of the contacts [17]. The main consequence is the existence of force chains and weakly loaded contacts in the assembly [24,45–49]. The effects of disorder are reduced here by the external loading applied on the crystal, a weak polydispersity in the diameter of the beads, and the controlled dimensions of the container. An important role is also played by the averaging of the signals over the transducer's surface, which diameter is $D = 2.5$ cm and is much larger than the diameter of the beads. Then, the measurements weakly depend on a precise configuration of the crystal inducing a specific network of force chains which is not reproducible. The results exposed below are reproducible. The elastic waves propagate in the direction perpendicular to the hexagonal layers, i.e., the z direction. The earlier experiments on linear acoustic propagation [19] in this geometry have been successfully correlated with the theoretical expectations. In this direction of propagation, the theory predicts the propagation of one pure longitudinal mode L, one pure rotational mode R, two coupled transverse and rotational modes TR and RT [18,19]. The dispersion relations of these modes along this direction of propagation are exposed in Fig. 2. The dispersion relations are developed in the reciprocal space (k_x,k_y,k_z) from the point $\Gamma = (0,0,0)$ to the point $2A = (0,0,\sqrt{3/2}\pi/a)$ [19].

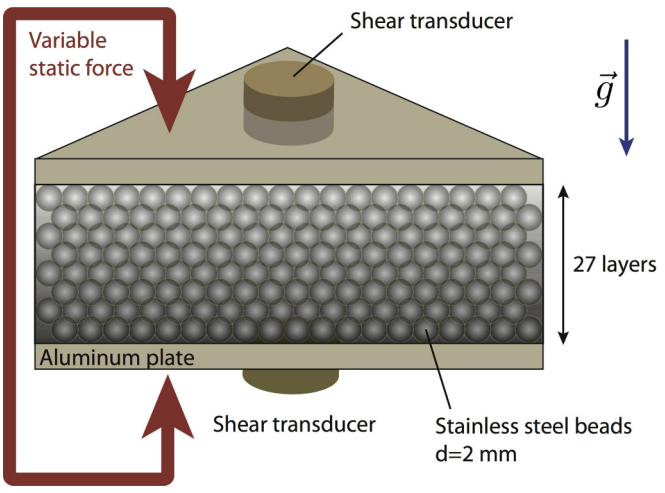

FIG. 1. (Color online) Sketch of the experimental setup.

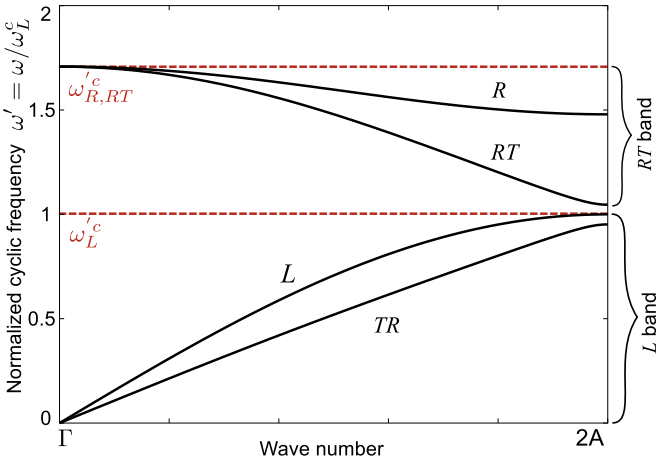

FIG. 2. (Color online) Dispersion relations of the bulk modes in a hcp granular crystal along the z direction. The cyclic frequencies are normalized with the cutoff frequency ω_L^c of the longitudinal mode L.

TABLE I. Cutoff frequencies at the top and the bottom of the crystal for the applied static loadings.

Applied static force per contact (mN)	F_L^c at the top (kHz)	F_L^c at the bottom (kHz)	F_{RT}^c at the top (kHz)	F_{RT}^c at the bottom (kHz)
2	60.4	69.0	103	118
5	70.4	75.2	120	128
10	79.0	81.9	135	140
15	84.5	86.7	144	148
20	88.7	90.4	151	154
25	92.1	93.5	157	160

The cutoff cyclic frequency of the longitudinal mode is [18]

$$\omega_L^c = \{[2(2+\Delta_K)(3aN_0)^{1/3}E^{2/3}]/[m_b(1-\nu^2)^{2/3}]\}^{1/2}, \quad (1)$$

where m_b is the mass of one bead, N_0 is the static normal force applied on each of the contacts, E and ν are the Young's modulus and Poisson's ratio of the material constituting the beads, respectively, and $\Delta_K = 2(1-\nu)/(2-\nu) = K_S/K_N$ is the ratio of shear K_S to normal K_N rigidities of the contact [28,29]. The cutoff frequency of the mode RT, which is the highest cutoff frequency for bulk mode propagation, is given by $\omega_{RT}^c = [10\Delta_K/(2+\Delta_K)]^{1/2}\omega_L^c$. Experimental results have confirmed the validity of this modelization [19]. The cutoff frequencies of the longitudinal mode $F_L^c = \omega_L^c/(2\pi)$ and the rotational-transverse mode $F_{RT}^c = \omega_{RT}^c/(2\pi)$ can be predicted in our system and are summarized in Table I.

Two frequency ranges can be distinguished (see Fig. 2). The translational frequency band, where propagate the longitudinal mode L and the transverse mode modified by the rotation TR, is called here the L band and is defined from 0 to F_L^c. The rotational frequency band, where propagate the rotational mode R and the rotational-transverse mode RT, is called here the RT band and is defined from F_L^c to F_{RT}^c. There are no modes propagating in the rotational frequency band if the rotational degrees of freedom of the individual beads are not taken into account.

The shear transducers have been used in the experiments because, being nominally shear, they are also emitting longitudinal wave, and are sufficiently sensitive in their detection [19]. Thus, they can be used to explore all the longitudinal and coupled rotational-transverse modes. It is assumed that the shear transducers can neither excite nor detect the pure rotational mode R. The variations of the relative importance of the longitudinal and shear waves in the performance of these transducers have been characterized by us through measurements of the signal emitted by a shear transducer and transmitted through an aluminum block using either a shear or longitudinal detecting transducer as exposed in Fig. 3. The longitudinal transducer is sensitive only to the longitudinal waves [19].

In the experiments described below, the burst source signal is a sine modulated in amplitude by a Gaussian envelope with a width of 3.5 kHz at −3 dB. The central frequency increases from 40 to 200 kHz by steps of 2.5 kHz. The transmitted amplitude is measured on the other side of the crystal by a shear transducer, which is the same model as the one used for the excitation. Specifically for the studies of the directional asymmetry or symmetry in wave propagation, the emitted and detected amplitudes from the two exploited transducers have been checked to be equal through additional experiments with a third transducer. Moreover, switching the two transducers leads to similar experimental results. Then, the measurements are carried out twice with two different paths of propagation. In the first path of ↑-propagation, the excitation is at the bottom of the crystal and the detection is at the top. In the second path of ↓-propagation, the excitation is at the top of the crystal and the detection at the bottom. Specifically for the studies of the nonlinear demodulation processes, the source signal is filtered with a high-pass filter to ensure that there are no low frequency components in the electric signal exciting the transducer.

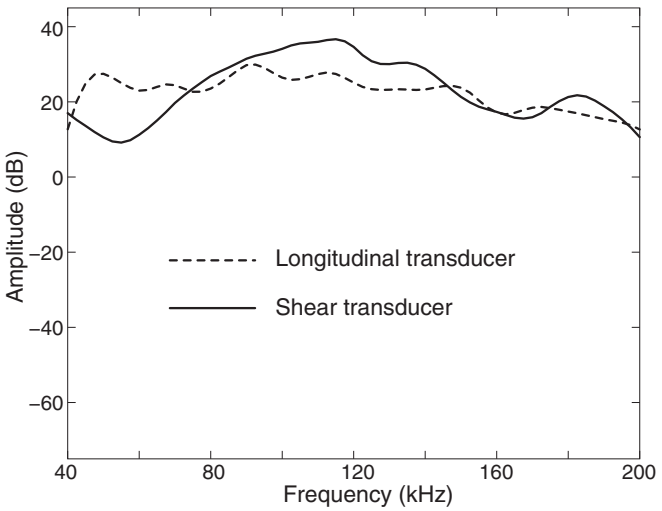

FIG. 3. Transmission through an aluminum block with a shear transducer in excitation and either a shear (continuous line) or a longitudinal (dashed line) transducer in detection.

III. EXPERIMENTAL OBSERVATIONS

Our measurements demonstrate that nonlinear acoustic phenomena in noncohesive granular crystals are important and, similarly to disordered granular media, can be directly assessed experimentally. In Fig. 4, we present as an illustration the spectrum of the signal transmitted through a granular crystal in comparison to a signal transmitted through an aluminum block, which is estimated to behave linearly at the considered excitation levels. The comparison in Fig. 4 clearly demonstrates the nonlinear acoustic processes of second harmonic generation and demodulation or rectification.

In the experiments devoted to the studies of the directional asymmetry in acoustic propagation through the three-dimensional granular crystal, we measured the amplitudes of the fundamental wave and of the demodulated wave as a function of the central frequency of the pump wave packet. The amplitude of the demodulated wave is measured as a difference between the amplitudes of the first two phases of opposite polarity in the low frequency acoustic pulse arriving on the detecting transducer. The form of the demodulated wave and its arrival time, which is estimated to correspond to the arrival time of the longitudinal mode at low frequencies,

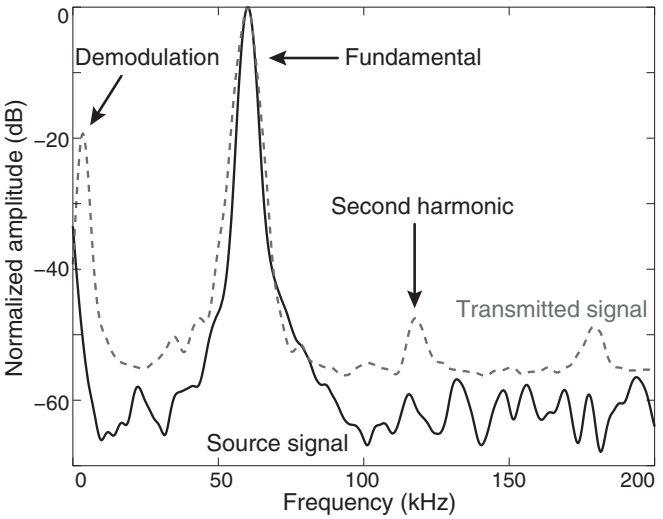

FIG. 4. Examples of the amplitude of the spectra of the source signal (black continuous line) and transmitted signal (gray dashed line) with the identification of linear and nonlinear wave propagation in the case of an excitation with a central frequency at 60 kHz. The second harmonic component is here visible at 120 kHz. The maximum amplitude component of the demodulated wave is found around 3 kHz.

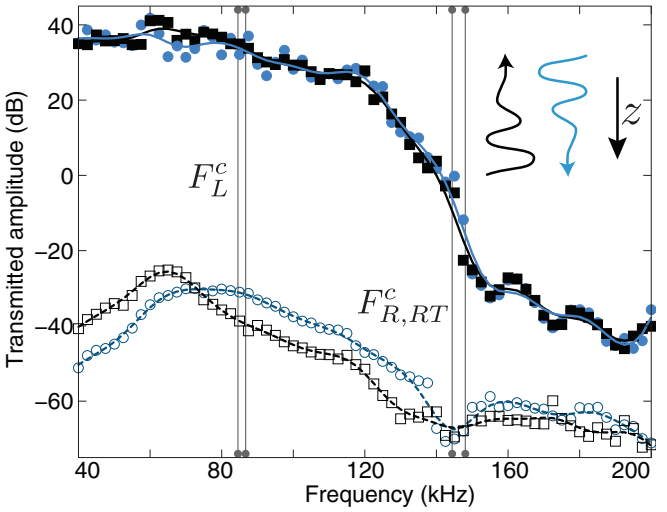

FIG. 5. (Color online) Transmitted amplitude of the linear (continuous curves and filled markers) and demodulated (dashed curves and empty markers) waves as a function of the central frequency of the excitation for a 15-mN static loading applied on the contacts at the top of the crystal. Propagation from the bottom to the top in black squares, from the top to the bottom in blue circles. The markers correspond to the experimental data, the curves correspond to a smoothed interpolation of the experimental results. The vertical curves represent the cutoff frequencies of the modes L and RT at the top and the bottom of the crystal.

weakly change with the central frequency of the pump wave confirming the nonlinear generation of low frequency longitudinal wave by high frequency pump waves. It is worth noting that determining the amplitude of the demodulated wave from spectral measurements, as those depicted in Fig. 4, leads to similar results.

In Fig. 5, we present the results of the asymmetry measurements conducted in the case of a 15-mN static loading applied on each of the contact between the beads at the top of the granular crystal. The vertical lines indicate the positions of the cutoff frequencies of the longitudinal and rotational-transverse acoustic modes estimated for the static loadings at the top and the bottom of the crystal.

The basic experimental observations can be summarized as follows. First, the amplitude of the signal at the fundamental frequency does not depend on its propagation direction at all tested frequencies, i.e., in complete L and RT bands and also in the evanescent regime of waves penetration above F_{RT}^c. We believe that the theoretically predicted forbidden band gap between F_L^c and the lowest frequency of propagation of the mode RT is not visible here because of the width of this band gap, which is comparable with the frequency width of the source signal. Second, the parametric emission is found to be practically always directionally asymmetric, i.e., the detected amplitude of the demodulated wave from the (downward) $\downarrow$-propagating pump wave packet is nearly always different from the one from the (upward) $\uparrow$-propagating pump wave packet. The sign of the directional asymmetry changes at a critical frequency belonging to the L band. Above this critical frequency, the parametric antenna operating from the top of the crystal is more efficient than the one operating from the bottom. Below this critical frequency, the situation is opposite.

These basic observations are qualitatively reproduced with other external static loadings, with an expected shift of all the characteristic frequencies with pressure. As an illustration, we present in Fig. 6 the dependence of the asymmetry of the nonlinear demodulation phenomenon on pump frequency at different static loadings. Asymmetry is measured by the

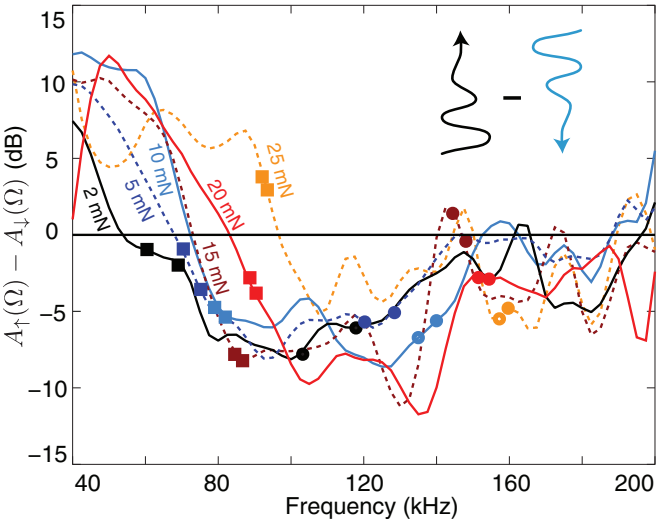

FIG. 6. (Color online) Difference of the amplitudes of the demodulated waves from the two paths of propagation, from the bottom to the top minus from the top to the bottom, in function of the central frequency of the excitation and for different static loading applied on the top of the crystal. The squares represent F_L^c at the top and the bottom of the crystal. The circles represent F_{RT}^c at the top and the bottom of the crystal.

difference of the amplitude of the demodulated wave emitted by the ↑-propagating pump wave and the one emitted by the ↓-propagating pump wave. The frequency of the crossing point, where the amplitudes of the demodulated waves from the two paths of propagation are equal, moves with the static loading ensuring that these observations come from the granular medium behavior.

IV. THEORETICAL INTERPRETATIONS

From the experimental results, we can observe that the propagation of the high frequency pump wave packets is much more directionally symmetric than the low frequency parametric emission by the pump waves. This observation is mostly related to a much lower sensitivity to pressure variations of the linear acoustic effects compared to the nonlinear ones. As a consequence, it is also related to the spatial inhomogeneity of pressure distribution within the granular packing. In particular, the linear processes of diffraction, refraction, and scattering depend on the wavelength λ, which is proportional to the acoustic phase velocity c_{ph}, e.g., $\lambda \propto c_{ph}$, and the phase velocity weakly depends on the static pressure p in granular media. In classic Hertzian model of contact [28,29], $c_{ph} \propto p^{1/6}$. In contrast, the acoustic parameter ε of quadratic elastic nonlinearity, to which the amplitude of the parametric emission is directly proportional, varies much faster with pressure change, $\varepsilon \propto p^{-2/3} \propto c_{ph}^{-4}$.

A. Directional symmetry of the linear propagation

It is instructive to estimate the possible directional asymmetry of the linear acoustic wave packets emitted and detected by equivalent transducers. The acoustic impedance of the used piezoceramic transducers is much higher than the acoustic impedance of the granular crystal. From the density of stainless steel $\rho_{\text{steel}} = 7780$ kg m^{-3} and the compacity of the hexagonal close-packed packing $\eta = 0.74$, the density ρ of our granular crystal is $\rho = 5760$ kg m^{-3}. It is practically independent of pressure for the pressure variations involved in our experiments. Thus, the acoustic impedance varies proportionally to the pressure as $c_{ph} \propto p^{1/6}$. For the highest velocities of the acoustic waves $c_{ph} \sim 500$ m s^{-1}, measured and theoretically estimated for the highest experimental static loadings, the acoustic impedance $Z = \rho c_{ph}$ is smaller than 3.10^6 kg m^{-2} s^{-1}, i.e., about an order of magnitude smaller than the impedance of the ceramic transducers. In this case, assuming a perfect elastic contact between the transducer and the granular crystal, the transmission of the acoustic displacement from the emitting transducer to the granular crystal does not depend on the impedance of the crystal, while the transmission from the granular crystal into the receiving transducer is proportional to the crystal impedance and thus is proportional to $p^{1/6}$. It should also be taken into account that the amplitude of the acoustic wave varies when it propagates in an inhomogeneous medium. In the frame of geometrical acoustics [50,51], the displacement amplitude scales in inhomogeneous medium of constant density as $\propto c_{ph}^{-1/2}$. Consequently, it scales as $\propto c_{ph}^{-1/2} \propto p^{-1/12}$ in the granular crystal. So the theory predicts, for instance, that the amplitude of the ↓-propagating wave will diminish in its in-depth propagation but this diminishing will be overcompensated by its better transmission into the receiving transducer at the bottom of the crystal, which is subjected to higher pressure. As a result, the amplitude $A_\downarrow(\omega)$ of the detected ↓-propagating wave scales as $A_\downarrow(\omega) \propto [p(z=H)/p(z=0)]^{-1/12} p^{1/6}(z=H)$, while the detected ↑-propagating wave scales as $A_\uparrow(\omega) \propto [p(z=0)/p(z=H)]^{-1/12} p^{1/6}(z=0)$. Here, $z=0$ and $z=H$ are the vertical coordinates of the top and bottom surfaces of the granular crystal, respectively. This leads to the theoretical expectation of weak directional asymmetry of the linear acoustic wave, $A_\downarrow(\omega)/A_\uparrow(\omega) \propto [p(z=H)/p(z=0)]^{1/6}$. The highest pressure ratio, of about 2, between the bottom and the top of the crystal is achieved in our experiment at the lowest static loading. Even in this limiting case, the theoretical prediction is $A_\downarrow(\omega)/A_\uparrow(\omega) \simeq 1.1 \simeq 1$ dB. It is also worth mentioning here that possible spatial inhomogeneity of the linear absorption does not contribute to the asymmetry of linear propagation, because the decrease in wave amplitude along the propagation from the emitter to the receiver depends on the integral of the absorption coefficient along this path of propagation. This integral does not depend on the direction of propagation.

We conclude this subsection with the statement that the experimentally observed directional symmetry at the pump frequency (see Fig. 5) can be interpreted as an evidence of the linear propagation of acoustic waves.

B. Directional asymmetry of parametric emission with mode conversion

In this subsection, we interpret the experimental results on parametric emission by the wave packets with pump frequencies above F_L^c, i.e., in the RT band. First, it is worth mentioning that the important fall in the parametric emission efficiency in the vicinity of the top of the RT band and above this propagating band, i.e., in the case where all the excited acoustic modes are evanescent (see Figs. 2 and 5), is in accordance with earlier theoretical predictions for granular crystals [43].

1. Mode conversion

In the RT band, the parametric emission has several features. First, the frequency down-conversion takes place in parallel with mode conversion. The emitted rotational-transverse waves, which represent the only propagating mode in this frequency band, are mode-converted into a longitudinal wave, which is the mode of propagation of the demodulated wave as argued in Sec. III. Earlier, in the nonlinear processes of shear waves mode-conversion into longitudinal, both demodulation [24] and the second harmonic generation [23] were observed in disordered granular packings. They were attributed to nonlinear dilatancy of the granular media [24]. In the current experiments in granular crystals, the growth of the amplitude of the demodulated signal is proportional to the square of the excitation amplitude under the majority of the experimental conditions. Thus, the quadratic nonlinear dilatancy is predominantly observed [24]. As an illustrative example, we present in Fig. 7 the measurements conducted in the case of a 20-mN static loading at a pump frequency of 120 kHz, which is in the RT band.

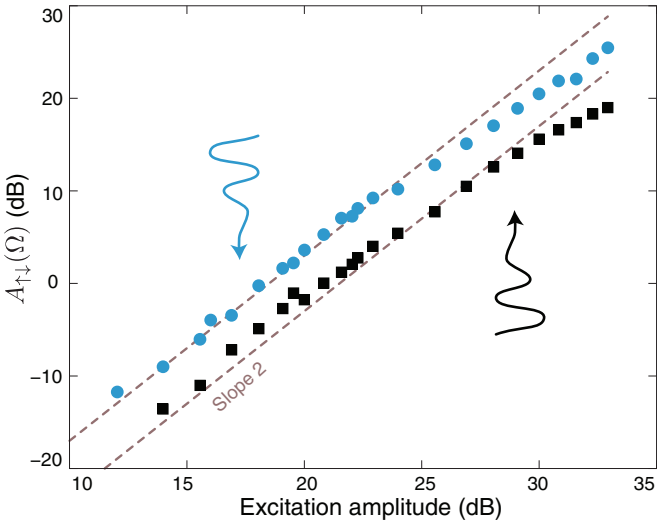

FIG. 7. (Color online) Dependence of the amplitude of the demodulated wave on the excitation amplitude with a central pump frequency of 120 kHz and a static loading of 20 mN per contact. The central frequency of the pump wave belongs to the RT band.

Second, in contrast to the previous experiments on nonlinear dilatancy [23,24], the nonlinear process is accompanied by band conversion. The high frequency pump waves belong to the RT band while the demodulated signal belongs to the L band.

2. Asynchronism

In the presentation of the phononic band in Fig. 2, the pump wave packets have negative group velocities and positive phase velocities. In reality, the situation is just opposite: the pump wave packets have negative phase velocities but positive group velocities. The corresponding point belongs to the symmetric part $\omega(\mathbf{k}) = \omega(-\mathbf{k})$ of the complete dispersion structure, which is not reproduced in Fig. 2. For the energy conserving demodulation process $\omega_1 - \omega_2 = \Omega$, with high carrier frequencies $\omega_1 > \omega_2 \equiv \omega$ and low demodulated cyclic frequency $\Omega \ll \omega$, the momentum conservation requirement $k(\omega_1) - k(\omega_2) = k(\Omega)$ can be approximated by the equality of the group velocity of the wave packet and the phase velocity of the demodulated wave, $c_{gr}(\omega) = c_{ph}(\Omega)$ [43]. As it follows from the dispersion relations for the experimental granular crystal (Fig. 2), the latter condition cannot be fulfilled and, thus, the demodulation process is importantly asynchronous, especially in the upper part of the RT band. The characteristic length of synchronism can be estimated from the condition $\Delta k L_{\text{syn}} = \pi/2$ [52,53], where $\Delta k \equiv |k(\omega_1) - k(\omega_2) - k(\Omega)| \cong \Omega|1/c_{gr}(\omega) - 1/c_{ph}(\Omega)|$ is the mismatch of the wave vectors. Thus, $L_{\text{syn}} = [\lambda(\Omega)/4]/|1 - c_{ph}(\Omega)/c_{gr}(\omega)|$, where λ is the wavelength. The estimates for the typical low frequency of 3 kHz and typical longitudinal velocity of 300 m s^{-1} predicts that the synchronism length is twice shorter than the thickness of the crystal already for $c_{gr}(\omega) \approx c_{ph}(\Omega)/2$. Closer to the top of the RT band, the synchronism length is much shorter than the crystal thickness. We believe that it is the synchronism length which controls the effective length of the parametric emitting antenna in the upper part of the RT band and which importantly influences the performance in the lower part of this frequency band, and even at the top of the L band.

3. Sign of asymmetry

For fixed amplitude of the pump wave packets, the amplitude of displacement in the nonlinearly emitted demodulated wave is proportional to the nonlinear acoustic parameter and the length of the parametric antenna, $A \propto \varepsilon L$ [38,39,43,50]. When the length of the parametric antenna, i.e., the length of effective amplification of low frequencies by the high acoustic frequencies, is controlled by the synchronism length, $L \propto L_{\text{syn}}$, which weakly depends on pressure through the weak influence of pressure on the linear acoustic velocities, the pressure influences the parametric emission mostly through its influence on the nonlinear acoustic parameter. Thus, the experimental detection of the larger amplitudes of the demodulated waves emitted by $\downarrow$-propagating wave packet rather than by $\uparrow$-propagating wave packet, $A_{\downarrow}(\Omega) > A_{\uparrow}(\Omega)$, can mostly be attributed to the dependence of the nonlinear acoustic parameter ε on pressure. The granular crystal in the gravity field is more nonlinear near its top than near its bottom, because the nonlinearity increases with diminishing pressure. We conclude this subsection with the statement that the negative sign in Fig. 6 of the directional asymmetry for the demodulation in the rotational band, $A_{\uparrow}(\Omega) - A_{\downarrow}(\Omega) < 0$, is not surprising but is rather expectable.

C. Directional asymmetry of parametric emission without mode conversion

The interpretation of the experimental observations in the case of the pump waves belonging to the lower part of the L band should include an explanation of the change of the sign in the directional asymmetry of the parametric emission, $A_{\uparrow}(\Omega) - A_{\downarrow}(\Omega) > 0$, relative to the observations in the RT band, $A_{\uparrow}(\Omega) - A_{\downarrow}(\Omega) < 0$, explained above.

1. Without mode conversion

In the L band, the longitudinal waves can propagate. In the lower part of this propagating band, considering the propagation of longitudinal waves, the synchronism condition is closer to fulfillment than in the above analyzed case of pump waves belonging to the RT band. The transverse-rotational mode TR of the L band propagates with a group velocity close to the one of the rotational-transverse mode RT of the RT band [18]. Therefore, the demodulation process with transverse pump waves is importantly asynchronous as in the case of pump waves belonging to the RT band. The cumulative character of the nonlinear processes is possible in the L band because of the synchronism between the longitudinal pump waves and the longitudinal demodulated pump wave. The contribution of the transverse-rotational waves to the nonlinear processes is assumed to be negligible. Thus, we interpret the nonlinear processes observed in the lower part of the L band as being mostly the processes involving the interaction of the longitudinal waves only, i.e., without mode conversion. This hypothesis is also supported by the experimental evaluation of the amplitude dependence

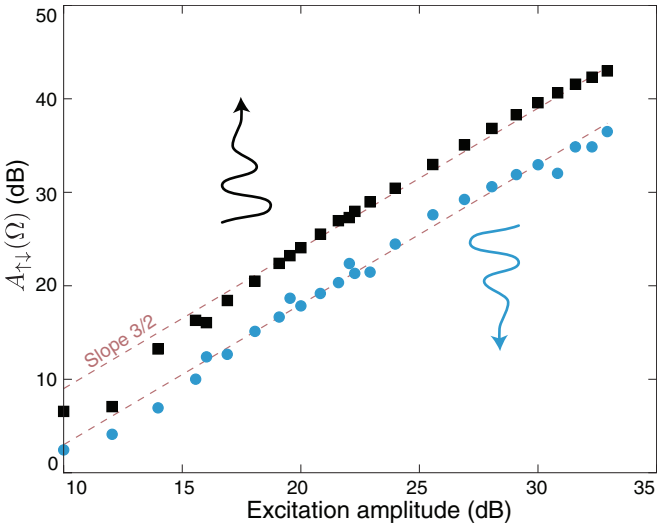

FIG. 8. (Color online) Dependence of the amplitude of the demodulated wave on the excitation amplitude with a central pump frequency of 60 kHz and a static loading of 20 mN per contact. The central frequency of the pump wave belongs to the L band.

of the demodulated wave on the wave packet amplitude. In the current experiments in granular crystals, the amplitude growth of the demodulated wave, emitted by wave packets with pump frequencies sufficiently lower than the cutoff frequency of the longitudinal mode, is proportional to the power 3/2 of the excitation amplitude under the majority of experimental conditions. Thus, the nonlinearity related to clapping-tapping regime of Hertzian contacts between the spherical grains [16,24,25] is predominantly observed. As an illustrative example, we present in Fig. 8 the measurements conducted in the case of 20 mN static loading per contact at a pump frequency of 60 kHz, which is in the L-band. This type of nonlinear behavior has been earlier mostly observed for the interactions between longitudinal acoustic waves (see Refs. [16,24] and the reference therein).

2. *Clapping nonlinearity*

The clapping nonlinearity of contacts is a strong nonanalytic nonlinearity, which exists when the amplitude of the acoustic wave is sufficient to overcome the local static loading of the contact and to drive the contact periodically between the open and the closed states. The 3/2 power dependence of the three-wave-mixing process is characteristic to the clapping of classic Hertzian contacts [16,24,29]. For the expected acoustic displacement amplitudes of the order of 0.5–5 nm, the acoustic strain η at a typical frequency of 60 kHz in the lower part of the first propagating frequency band is estimated to be of the order of $\eta \propto 10^{-7}$–10^{-6}. This order of magnitude is insufficient to open the intergrain contacts in the granular crystal, which are estimated to be statically preloaded in our experiments in average by the strain of $\eta_0 \propto 10^{-5}$. This estimate is done for the Hertzian contacts, for which $\eta_0 \approx K^{-2/3}(a/2)^{-4/3}N_0^{2/3}$, where $K \equiv (4/3)[E/(1-\nu^2)]$ denotes the effective modulus [29,33]. Thus, the observation of 3/2 power law in our nonlinear acoustic experiments in three-dimensional granular crystal demonstrates that, in ordered granular assemblies, similarly to the documented observations for disordered granular media (see [24] and the reference therein), there is an important fraction of weak contacts, which are statically preloaded much weaker than in average. In compensation, a fraction of contacts, which are loaded stronger than the average and are forming force chains, is also expected in granular media [24,45–49].

3. *Sign of asymmetry*

Following the discussion in Sec. IV B, the explanation of the particular directional asymmetry $A_{\uparrow}(\Omega) - A_{\downarrow}(\Omega) > 0$ in parametric emission in the lower part of the L band cannot be based on the inequality $\varepsilon(z=0) > \varepsilon(z=H)$. Thus, an important role in the documented asymmetry is played by the change in the effective length of the parametric antenna when the direction of the pump propagation changes. For the quasisynchronous processes of demodulation without mode conversion, the length of synchronism importantly exceeds the crystal thickness and cannot be the scale which limits the effective length of parametric emission. The characteristic diffraction length $L_{\rm diff}(\omega) \propto D^2/\lambda(\omega)$ of the wave packets also importantly exceeds the crystal thickness. At a typical frequency of 60 kHz, we have estimated that $L_{\rm diff}(\omega) \geqslant 3H$, for instance. Under these circumstances, the length of the parametric antenna will be controlled by the attenuation length $L_{\rm att}(\omega)$ of the high frequency carrier waves [38,42].

As follows from the above discussion, a rather broad spectrum of contact static loadings could be expected and, thus, the attenuation of the wave packets can be caused both by their absorption and their scattering due to the residual disorder persisting in the granular crystal even under external loading. Neglecting the possible contribution to the parametric emission from scattered high frequency waves, i.e., accounting only for the parametric emission by ballistic waves [42], the condition, which is necessary for the realization of the observed directional asymmetry, can be qualitatively written in the form $L_{\rm att}(\omega,z=0)\varepsilon(z=0) < L_{\rm att}(\omega,z=H)\varepsilon(z=H)$. Qualitatively speaking, if the decrease of the acoustic nonlinearity is overcompensated by the increase in the high frequency attenuation length, the demodulated acoustic signal emitted by the $\uparrow$-propagating wave packets will be larger in amplitude than the one emitted by the $\downarrow$-propagating wave packets. Speaking differently, the positive sign in the directional asymmetry of the parametric emission in the lower part of the L band is a manifestation of higher spatial inhomogeneity of the acoustic attenuation in comparison with inhomogeneity of the nonlinear parameter. The fact that both acoustic absorption and scattering diminish with increasing pressure that reduces the portion of mobilized or sliding contacts and also reduces disorder, is well known. However, the evaluation of the possible functional dependence of the absorption and scattering on static pressure remains an open question and is far beyond the scope of the present paper. A bit more elaborate theory of the parametric emission, which, in contrast to the proposed above inequality $L_{\rm att}(\omega,z=0)\varepsilon(z=0) < L_{\rm att}(\omega,z=H)\varepsilon(z=H)$, accounts for the spatial distribution of the acoustic absorption and nonlinearity between the top and the bottom of the crystal, is presented in the next section.

V. ADVANCED THEORETICAL MODEL

A. Model description

In this section, assuming the one-dimensional propagation of a wave in a granular medium, the following model can be considered to evaluate the amplitude of the nonlinear demodulated wave as a function of the direction of propagation. The two parameters involved in the amplitude of the acoustic waves are the in-depth dependence of the nonlinear parameter $\varepsilon(z)$ and the in-depth distribution of the attenuation $\alpha(z)$. The amplitude of the pump wave $A(\omega)$ can be written as

$$A(\omega,z) = A(\omega,0)e^{-\int_0^z \alpha(z')dz'}. \tag{2}$$

Considering, for a compact illustration of the physical principle, the demodulated wave as consequence of the quadratic nonlinear elastic behavior of the medium and using the successive approximation method, the pump wave is the source of the demodulated wave. Therefore, the amplitude $A(\Omega)$ of the demodulated wave grows as

$$\frac{\partial A(\Omega)}{\partial z} \sim [A(\omega,0)]^2\varepsilon(z)e^{-2\int_0^z \alpha(z')dz'}. \tag{3}$$

Because the amplitudes of the wave packets emitted from the top and the bottom of the crystal are equal (see Sec. IV A), then the dependence on the wave amplitude in Eq. (3) can be omitted for the evaluation of the directional asymmetry of the parametric emission. The amplitude of the demodulated wave when the propagation is in the direction of gravity (from the top to the bottom) can be written as

$$A_\downarrow(\Omega) \sim \int_0^H \varepsilon(z)e^{-2\int_0^z \alpha(z')dz'}dz. \tag{4}$$

The amplitude of the demodulated wave when the propagation is in the direction opposite of gravity (from the bottom to the top) can be written

$$A_\uparrow(\Omega) \sim -\int_H^0 \varepsilon(z)e^{2\int_H^z \alpha(z')dz'}dz. \tag{5}$$

Finally, the comparison of the amplitudes of the demodulated waves from the two directions of propagation provides the following estimate for the directional asymmetry of parametric emission:

$$A_\uparrow(\Omega) - A_\downarrow(\Omega) \sim \int_0^H \varepsilon(z)[e^{-2\int_z^H \alpha(z')dz'} - e^{-2\int_0^z \alpha(z')dz'}]dz. \tag{6}$$

Simple models can be used for $\varepsilon(z)$ and $\alpha(z)$ using three characteristic lengths, the length of linear attenuation L_{att}, the length of inhomogeneity of the linear attenuation $L_{\text{att}}^{\text{inh}}$, and the length of inhomogeneity of nonlinearity L_{NL}^{inh}. The in-depth dependence of the attenuation parameter could be approximated by

$$\alpha(z) = \frac{1}{L_{\text{att}}}\left(1 - \frac{z}{L_{\text{att}}^{\text{inh}}}\right). \tag{7}$$

This model assumes that $L_{\text{att}}^{\text{inh}} \geqslant H$, and, in particular, it assumes that $L_{\text{att}}^{\text{inh}}$ is positive, i.e., attenuation diminishes with depth as could be expected theoretically (see Sec. IV C).

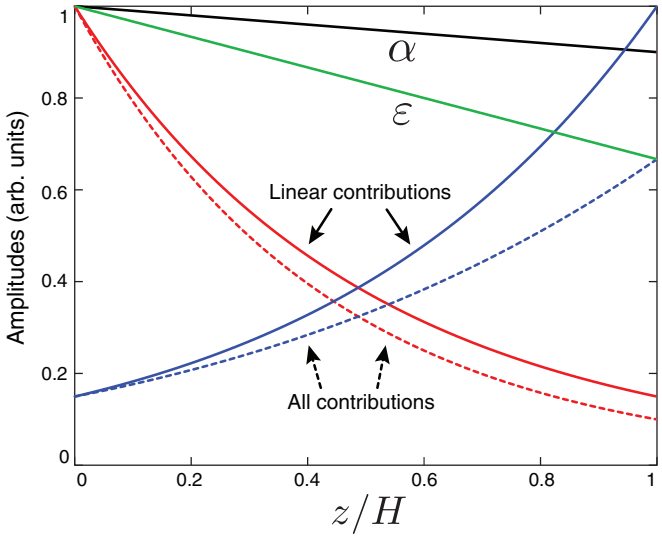

FIG. 9. (Color online) Example of calculation of $\alpha(z)$, $\varepsilon(z)$, $e^{-\int_0^z \alpha(z')dz'}$ (blue and red lines), and $\varepsilon(z)e^{-2\int_0^z \alpha(z')dz'}$ (blue and red dashed lines) over z to visualize the evolution of the functions inside Eq. (3) following the two paths of propagation.

The in-depth dependence of the nonlinear parameter could be approximated by

$$\varepsilon(z) \propto 1 - z/L_{NL}^{\text{inh}}. \tag{8}$$

This assumes that $L_{NL}^{\text{inh}} \geqslant H$ and that the acoustic nonlinearity is diminishing with depth as is known from the earlier experiments and theoretical models (see Sec. IV B). The evolutions with z of $\alpha(z)$, $\varepsilon(z)$, $e^{-\int_0^z \alpha(z')dz'}$, and $\varepsilon(z)e^{-2\int_0^z \alpha(z')dz'}$ are shown in Fig. 9. Including (7) and (8) in (6), the comparison of the demodulated wave amplitude from the two directions of propagation requires the evaluation of the function difference $\psi(L_{\text{att}}, L_{\text{att}}^{\text{inh}}, L_{NL}^{\text{inh}})$ defined with

$$\begin{aligned} A_\uparrow(\Omega) - A_\downarrow(\Omega) &\sim \psi\left(L_{\text{att}}, L_{\text{att}}^{\text{inh}}, L_{NL}^{\text{inh}}\right) \\ &= \int_0^H \left(1 - \frac{z}{L_{NL}^{\text{inh}}}\right)\left[e^{-2(H-z+(z^2-H^2)/2L_{\text{att}}^{\text{inh}})/L_{\text{att}}}\right. \\ &\quad \left. - e^{-2(z-z^2/2L_{\text{att}}^{\text{inh}})/L_{\text{att}}}\right]dz. \end{aligned} \tag{9}$$

B. Results and discussion

The condition $\psi = 0$ is exposed in Fig. 10 as a function of the three parameters L_{att}, L_{NL}^{inh}, and the ratio $L_{\text{att}}^{\text{inh}}/L_{NL}^{\text{inh}}$. Below the surface $\psi = 0$, the function ψ is positive. Above the surface $\psi = 0$, the function ψ is negative. Considering the function $\psi = 0$ along the L_{att}/H axis, it can be observed that the length of linear attenuation has an effect only if it is very small compared to length of propagation H of the problem. If $L_{\text{att}} > 10^{-2}H$, the function $\psi = 0$ will only depend on the values of $L_{\text{att}}^{\text{inh}}$ and L_{NL}^{inh}, and more precisely, it will depend mostly on the ratio $L_{\text{att}}^{\text{inh}}/L_{NL}^{\text{inh}}$.

Considering the function $\psi = 0$ along the L_{NL}^{inh} axis away from small values of L_{att}, i.e., $L_{\text{att}} > 10^{-2}H$, the function ψ can be equal to zero when $L_{\text{att}}^{\text{inh}}/L_{NL}^{\text{inh}} \simeq 1$. This means that

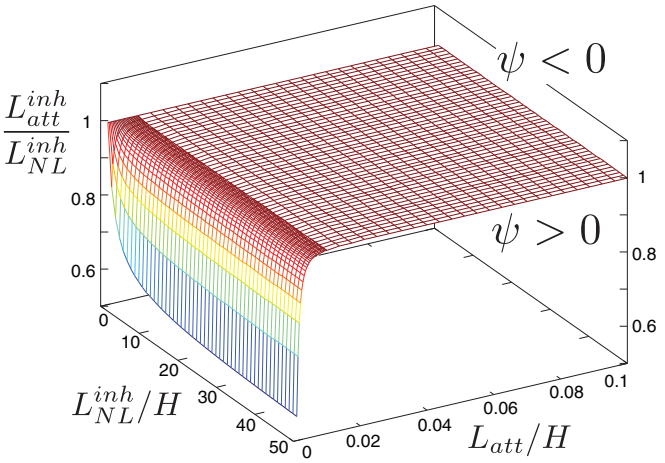

FIG. 10. (Color online) $\psi = 0$ with L_{att}, L_{NL}^{inh}, and the ratio $L_{\text{att}}^{\text{inh}}/L_{NL}^{\text{inh}}$.

the function ψ can be positive if $L_{\text{att}}^{\text{inh}} < L_{NL}^{\text{inh}}$. If L_{att} is very small, $L_{\text{att}} < 10^{-2}H$, meaning that the pump waves are very strongly attenuated at the top, the ratio $L_{\text{att}}^{\text{inh}}/L_{NL}^{\text{inh}}$ should be very small to get $\psi > 0$. A ratio $L_{\text{att}}^{\text{inh}}/L_{NL}^{\text{inh}} \ll 1$ represents an important drop of the attenuation with depth while the nonlinear behavior remains almost constant, the pump waves are almost evanescent at the top but can propagate at the bottom.

In conclusion, this theoretical model shows that, in the case of synchronism between the pump waves and the demodulated waves, the amplitude of the demodulated wave propagating from the bottom to the top can be larger than the amplitude of the demodulated wave propagating from the top to the bottom if the length of inhomogeneity of attenuation $L_{\text{att}}^{\text{inh}}$ is smaller than the length of inhomogeneity of nonlinearity L_{NL}^{inh}.

Formally, this model does not describe the case of an asynchronism between the pump and the demodulated wave. Nevertheless, the case where the asynchronism between the two waves is important can be analyzed, using this model, in a qualitative way. The first case that can be considered is the case of evanescent pump waves on both sides of the crystal. The central frequency of excitation is then above the highest cutoff frequency $F_{R,RT}^{c}$. In this case, the linear attenuation length tends to zero ($L_{\text{att}} \to 0$) and the length of linear attenuation inhomogeneity tends to infinity ($L_{\text{att}}^{\text{inh}} \to +\infty$), indicating that the attenuation of wave amplitude is due to the granular crystal periodicity, which is negligibly changed in depth under the conditions of our experiments. The nonlinear wave is then generated at the proximity of the source and since the medium has a larger nonlinearity at the top than at the bottom, the amplitude of the nonlinear wave generated in downward propagation is larger than in upward propagation, then $A_{\uparrow}(\Omega) - A_{\downarrow}(\Omega) < 0$. This result is valid since $L_{NL}^{\text{inh}} < +\infty$. This interpretation corresponds to the experiments when the demodulated wave is observable above the highest cutoff frequency.

When the synchronism length is small as in Sec. IV B, the nonlinear generation can be considered only at the beginning of the path of propagation, at the vicinity of the transducers. The further nonlinear generation process along the pump wave propagation can be neglected. This case could be modeled considering that the length of linear attenuation L_{att} in the above formulas models the role of L_{synch} and is small. From Fig. 10, the ratio $L_{\text{att}}^{\text{inh}}/L_{NL}^{\text{inh}}$ falls for small L_{att} to ensure that $\psi = 0$. This means that $L_{\text{att}}^{\text{inh}}$ needs to be much smaller than L_{NL}^{inh} to obtain $\psi > 0$. However, in the considered case of strong asynchronism, there is no inhomogeneity or asymmetry of the asynchronism (see Sec. IV B), meaning that $L_{\text{att}}^{\text{inh}} \gg H$. As a result, the condition $\psi > 0$ cannot be achieved in this case. Thus, our analysis demonstrates that $A_{\uparrow} - A_{\downarrow}$ will be always negative in the case where the pump waves and the demodulated waves are asynchronous.

VI. CONCLUSIONS

We studied the operation of the parametric emitting antenna in a three-dimensional noncohesive granular crystal under gravity. The asymmetry in parametric emission in a granular crystal is controlled by three features, the asynchronism of the linear and nonlinear waves due to periodicity of the structure, the nonlinearity, and the attenuation distribution in the medium depth. In the first case, the frequencies of the pump waves are above the highest cutoff frequency of the bulk modes of the granular crystal. The pump waves do not propagate, the attenuation of the pump waves is large and does not depend on the depth. The asymmetry in parametric emission is then controlled by the inhomogeneity of the acoustic nonlinear parameter. In the second case, the central frequencies of the pump wave packets belong to the second (rotational) propagating band. The demodulation, with mode conversion from the rotational-transverse acoustic modes into longitudinal mode in addition to the band conversion from the upper rotational frequency band to the lower longitudinal frequency band, is documented. The nonlinear frequency down-conversion process is importantly asynchronous and the observed directional asymmetry in parametric emission, along and opposite to the gravity direction, is attributed to the spatial vertical inhomogeneity in the distribution of the acoustic nonlinear parameter in the noncohesive granular crystal. In the last case, the central frequencies of the pump wave packet belong to the lower part of the first (longitudinal) propagating band of the phononic crystal. The demodulation can be attributed to nonlinear processes without mode conversion. In this case, the directional asymmetry in the parametric emission is of opposite sign to the asymmetry reported in the rotational frequency band. The directional asymmetry is then also controlled, in addition to the nonlinear parameter inhomogeneity, by the vertical inhomogeneity of the wave attenuation. From the theoretical predictions, the sign of the asymmetry observed in this case means that the attenuation falls faster than nonlinearity with increasing depth (or equivalently with increasing pressure). The experimental results also indicate that, even in ordered granular assemblies under a static preloading, there exists an important number of intergrain contacts, which are loaded much weaker than in average over the crystal and which can play an important role in the nonlinear acoustic phenomena. The research results reported here could be useful in the future to guide the design of spatially inhomogeneous nonlinear metamaterials for asymmetric propagation

of acoustic waves. Through their generalization to disordered granular assemblies, they could be also useful for better understanding of the relevant acoustic wave phenomena in geophysics.

ACKNOWLEDGMENTS

This research was conducted in the frame of the project "PROPASYM" (Pari scientifique 2013), supported by the Région Pays-de-la-Loire.

[1] V. F. Nesterenko, C. Daraio, E. B. Herbold, and S. Jin, Phys. Rev. Lett. **95**, 158702 (2005).
[2] B. Liang, B. Yuan, and J.-C. Cheng, Phys. Rev. Lett. **103**, 104301 (2009).
[3] B. Liang, X.-S. Guo, J. Tu, D. Zhang, and J.-C. Cheng, Nat. Mater. **9**, 989 (2010).
[4] N. Boechler, G. Theocharis, and C. Daraio, Nat. Mater. **10**, 665 (2011).
[5] A. A. Maznev, A. G. Every, and O. B. Wright, Wave Motion **50**, 776 (2013).
[6] R. Fleury, D. L. Sounas, C. F. Sieck, M. R. Haberman, and A. Alù, Science **343**, 516 (2014).
[7] J.-J. Chen, X. Han, and G.-Y. Li, J. Appl. Phys. **113**, 184506 (2013).
[8] S. Lepri and G. Casati, Phys. Rev. Lett. **106**, 164101 (2011).
[9] B. Liang, X.-Y. Zou, B. Yuan, and J.-C. Cheng, Appl. Phys. Lett. **96**, 233511 (2010).
[10] X.-F. Li, X. Ni, L. Feng, M.-H. Lu, C. He, and Y.-F. Chen, Phys. Rev. Lett. **106**, 084301 (2011).
[11] F. Gassmann, Geophysics **16**, 673 (1951).
[12] L. M. Schwartz, D. L. Johnson, and S. Feng, Phys. Rev. Lett. **52**, 831 (1984).
[13] M. de Billy, J. Acoust. Soc. Am. **108**, 1486 (2000).
[14] J. Anfosso and V. Gibiat, Europhys. Lett. **67**, 376 (2004).
[15] C. Inserra, V. Tournat, and V. Gusev, Europhys. Lett. **78**, 44001 (2007).
[16] V. Tournat and V. Gusev, Acta Acust. Acust. **96**, 208 (2010).
[17] A. Merkel, V. Tournat, and V. Gusev, Ultrasonics **50**, 133 (2010).
[18] A. Merkel, V. Tournat, and V. Gusev, Phys. Rev. E **82**, 031305 (2010).
[19] A. Merkel, V. Tournat, and V. Gusev, Phys. Rev. Lett. **107**, 225502 (2011).
[20] V. Tournat, I. Perez-Arjona, A. Merkel, V. Sanchez-Morcillo, and V. Gusev, New J. Phys. **13**, 073042 (2011).
[21] H. Pichard, A. Duclos, J.-P. Groby, V. Tournat, and V. E. Gusev, Phys. Rev. B **86**, 134307 (2012).
[22] H. Pichard, A. Duclos, J.-P. Groby, V. Tournat, and V. E. Gusev, Phys. Rev. E **89**, 013201 (2014).
[23] V. Tournat, V. E. Gusev, V. Y. Zaitsev, and B. Castagnède, Europhys. Lett. **66**, 798 (2004).
[24] V. Tournat, V. Zaitsev, V. Gusev, V. Nazarov, P. Béquin, and B. Castagnède, Phys. Rev. Lett. **92**, 085502 (2004).
[25] V. Tournat, C. Inserra, and V. Gusev, Ultrasonics **48**, 492 (2008).
[26] S. Sen, J. Hong, J. Bang, E. Avalos, and R. Doney, Phys. Rep. **462**, 21 (2008).
[27] A. Leonard and C. Daraio, Phys. Rev. Lett. **108**, 214301 (2012).
[28] J. Duffy and R. D. Mindlin, Tech. Rep. No. CU-TR-17 (Columbia University, New York, Dept. of Civil Engineering and Engineering Mechanics, 1956).
[29] K. L. Johnson, *Contact Mechanics* (Cambridge University Press, Cambridge, England, 1985).
[30] O. Mouraille, W. A. Mulder, and S. Luding, J. Stat. Mech.: Theory Exp. (2006) P07023.
[31] G. Theocharis, M. Kavousanakis, P. G. Kevrekidis, C. Daraio, M. A. Porter, and I. G. Kevrekidis, Phys. Rev. E **80**, 066601 (2009).
[32] C. Chong, P. G. Kevrekidis, G. Theocharis, and C. Daraio, Phys. Rev. E **87**, 042202 (2013).
[33] V. Gusev, V. Aleshin, and V. Tournat, Acta Acust. Acust. **94**, 215 (2008).
[34] V. E. Gusev, V. Aleshin, and V. Tournat, Phys. Rev. Lett. **96**, 214301 (2006).
[35] V. Aleshin, V. Gusev, and V. Tournat, J. Acoust. Soc. Am. **121**, 2600 (2007).
[36] X. Jacob, V. Aleshin, V. Tournat, P. Leclaire, W. Lauriks, and V. E. Gusev, Phys. Rev. Lett. **100**, 158003 (2008).
[37] V. Gusev and V. Tournat, Phys. Rev. E **78**, 036602 (2008).
[38] B. K. Novikov, O. V. Rudenko, and V. I. Timochenko, *Nonlinear Underwater Acoustics* (ASA, New York, 1987).
[39] A. Moussatov, V. Gusev, and B. Castagnède, Phys. Lett. A **283**, 216 (2001).
[40] V. Tournat, B. Castagnède, V. Gusev, and P. Béquin, C. R. Mecanique **331**, 119 (2003).
[41] V. Gusev, Acoust. Lett. **22**, 40 (2000).
[42] V. Tournat, V. E. Gusev, and B. Castagnède, Phys. Rev. E **66**, 041303 (2002).
[43] V. Tournat, V. E. Gusev, and B. Castagnède, Phys. Rev. E **70**, 056603 (2004).
[44] J. Cabaret, V. Tournat, and P. Béquin, Phys. Rev. E **86**, 041305 (2012).
[45] F. Radjai, M. Jean, J.-J. Moreau, and S. Roux, Phys. Rev. Lett. **77**, 274 (1996).
[46] T. S. Majmudar and R. P. Berhinger, Nature (London) **435**, 1079 (2005).
[47] O. Mouraille and S. Luding, Ultrasonics **48**, 498 (2008).
[48] E. T. Owens and K. E. Daniels, Europhys. Lett. **94**, 54005 (2011).
[49] M. Kramar, A. Goullet, L. Kondic, and K. Mischaikow, Phys. Rev. E **87**, 042207 (2013).
[50] L. M. Brekhovskikh and O. A. Godin, *Acoustics of Layered Media I: Plane and Quasi-plane Waves* (Springer-Verlag, Berlin, 1990).
[51] V. Gusev, A. M. Lomonosov, P. Ruello, A. Ayouch, and G. Vaudel, J. Appl. Phys. **110**, 124908 (2011).
[52] W. Lauterborn, T. Kurz, and M. Wiesenfeldt, *Coherent Optics, Fundamentals and Applications* (Springer-Verlag, Berlin, Heidelberg, 1993).
[53] M. Hamilton, Y. A. Il'inskii, and E. A. Zabolostkaya, in *Nonlinear Acoustics*, edited by M. F. Hamilton and D. T. Blackstock (Academic, San Diego, 1998), pp. 151–175.